

Compound formation under local thermal spikes during ion-beam mixing: Model and its experimental verification

Sankar Dhar,^{*} Y. N. Mohapatra,[†] and V. N. Kulkarni[‡]

Department of Physics, Indian Institute of Technology, Kanpur- 208016, India

(Received 27 November 1995; revised manuscript received 21 March 1996)

We propose a model to explain the experimentally observed ion-beam mixing rates in reactive systems under nonoverlapping spike conditions. There are several technologically important metal-semiconductor systems belonging to this class. For comparison with model prediction, we have studied experimentally ion-beam mixing in Cu/Ge bilayer systems at various temperatures. The results show that the room-temperature mixing rate varies linearly with deposited energy density F_D and that the mixing is a diffusion controlled process proceeding via compound formation. Excellent agreement has been obtained between the experimental observations and theoretical values predicted from our proposed model while other current models are seen to be inadequate. The model also explains the mixing rates of the Ni/Si system reported in the literature. [S0163-1829(96)01332-X]

I. INTRODUCTION

Among the directed energy deposition techniques, ion-beam mixing has been widely used for producing stable, metastable, and amorphous phases in metal/semiconductor¹⁻³ thin films at relatively lower temperatures than the corresponding thermal reactions.⁴ These phases have many potential applications in modern semiconductor industry for making contacts, interconnects, insulating layers, and protective coatings, etc.^{2,4} In order to make the ion-beam mixing a viable technique for the above-mentioned applications, the important prerequisite is the understanding of the physics behind the basic mechanisms for different processing conditions under which these phases synthesize. Some of the important parameters are mass, energy, flux, etc. of the incident ion and the thermodynamic parameters related to the mixing elements such as cohesive energy, heat of mixing, and substrate temperature.^{3,5} Several ion-beam mixing studies have been reported for metal/Si,^{1,3,6} metal/metal^{3,5,7-10} systems, which reveal the character of the mixing mechanism under different combinations of the above-mentioned conditions. From these studies it is now well established that for a given bilayer system of two elements, there exist two critical temperatures T_c (Refs. 5, 11, 12, and 14) and T_{eq} .¹² Below T_c , the mixing rate is independent of the temperature commonly referred to as the athermal mixing region.⁵ Above T_c the mixing rate becomes temperature dependent exhibiting a thermally activated region.^{11,13}

For irradiation temperatures T_c (Refs. 11, 12, and 14) or below, the mixing process is dominated either by the collision cascades^{3,15} or diffusion in thermal spikes coupled with the thermodynamic driving forces in a complex manner.^{1,3,5,7,8,10} In order to explain the experimental mixing rates of ion-beam mixing in this region, several phenomenological models have been proposed.^{5,7,9,10,11,15} These phenomenological models seek to predict the dependence of mixing on the deposition energy by the irradiating ions and ballistic parameters, i.e., atomic number, atomic density, mass, etc. of the target and incident ions. Also the under-

standing of such mechanisms have been enriched by the molecular-dynamics studies.^{11,16}

The ballistic model¹⁵ which uses the ballistic properties without considering the thermodynamic parameters is valid for elements with average atomic number $Z_{ave} < 20$ for low deposition energy, F_D of the irradiating ion into the target.^{5,11} Recently, Kelly and Miotello¹⁷ incorporated a chemically guided defect motion in their ballistic approach of ion mixing.

On the other hand, for elements with $Z_{ave} > 20$ exhibiting strong thermodynamic driving force, the rate of mixing is explained by models which consider the overlapping^{1,5,7} or nonoverlapping^{9,10,11} subcascades. The overlapping subcascade/global spike model of Johnson *et al.*⁷ predicts the mixing rate to be proportional to the square of the deposited energy density F_D . It has been successfully used in cases of high- Z target atoms and heavy irradiating ions for which the cascade density is expected to be large.^{3,5} However, recent experimental results^{8,9,10} show that for systems consisting of elements, the Z values of which lie in the range of $17 < Z_{ave} < 39$, mixing rate is generally proportional to F_D below a critical energy density F_D^{crit} .¹⁰ Borgesen, Lilienfeld, and Johnson⁹ and Bolse¹⁰ have explained this linear dependence by considering the mixing process within nonoverlapping subcascades/local spikes. As for example, in the case of the Ni/Ti system,⁸ the mixing rate varies linearly with F_D up to 7 keV/nm, whereas for the Co/Ti system, it varies up to 2.25 keV/nm. But when $F_D > F_D^{crit}$, the local spikes start to overlap on each other and form a single global spike.¹⁰ The overlapping occurs above 2.25 and 7 keV/nm for Co/Ti (Ref. 8) and Ni/Ti systems, respectively, and the probability of overlapping at lower F_D values increases with increasing Z values.

Recently, Desimoni and Traverse¹ have reported that the silicide formation occurs in Pd/Si and Ni/Si systems and the mixing rate varies linearly as a function of F_D^2 . For the Pd/Si system, the square of the mixed layer X^2 shows two different kind of dependence as a function of irradiation dose Φ . The dependence is quadratic ($X^2 \propto \Phi^2$) up to a critical dose Φ_c and

above this becomes linear ($X^2 \propto \Phi$) and is independent of irradiation temperature between 80–500 K.¹⁸ They have found that the calculated mixing rates using the Johnson and Cheng model^{5,7} are 3–8 times lower than the measured mixing rates and does not exhibit the observed quadratic dose dependence as well.^{1,18} However, they have found good quantitative agreement between calculated and experimental mixing rates by using a model in Ref. 1, which the chemical kinetics of compound formation enhances diffusion during mixing.

Their success motivates us to ask whether this model can be extended to the cases of mixing dominated by nonoverlapping subcascades, where compound formation also occurs. In fact, there are several compound forming systems^{1,2,6} (two of which will be discussed in this paper) consisting of elements with Z_{ave} in the range 17–39, where the mixing rate is proportional to F_D . However, the observed mixing rates in these cases are much higher than those calculated from local spike models,^{9,10} which also predict linear dependence of mixing rate with F_D as mentioned earlier. It is interesting to note that there are several technologically important metal/semiconductor systems such as Cu/Ge, Ni/Ge, Ni/Si, Y/Si, etc.,^{1,2,6} which belong to this category. For example, the copper germanide phase has emerged as an important material for contacts and interconnections for VLSI technology due to its unusually low resistivity of the order of few $\mu\Omega\text{-cm}$ and other favorable properties.^{2,19}

In the present work, we extend the model of Desimoni and Traverse¹ of compound formation to the cases where mixing occurs under nonoverlapping subcascades. The predictions of this model are shown to be in good agreement with the medium- Z bilayer compound forming systems where mixing rate is proportional to F_D . We also report a set of ion-beam mixing experimental results of the Cu/Ge system in detail. The Cu/Ge system has been chosen because it forms a Cu_3Ge compound at room temperature by ion-beam mixing, as has been shown by us recently for multilayer configuration.² Also, local spike formation is expected in this system, according to the criteria proposed by Cheng,⁵ Bolse,¹⁰ and Rossi and Nastasi.¹¹ These experimental results will be compared with the theoretical value predicted from the model proposed here, as well as with theoretical predictions of other current models. In addition, we will also show that the prediction of mixing rate from the proposed model is very close to the experimental results of a Ni/Si bilayer system reported in Ref. 1.

II. MODEL FOR COMPOUND FORMATION UNDER LOCAL SPIKES MIXING

It is now well recognized that thermodynamics has to be taken into account in describing ion-beam mixing and is normally manifests through heat of mixing. Johnson *et al.*⁷ and Cheng⁵ have shown that under regular solution approximation the diffusion coefficient can be expressed as

$$D = D_0(1 - 2\Delta H_{\text{mix}}/k_B T), \quad (1)$$

where D_0 is constant, k_B is Boltzman constant, and ΔH_{mix} is the heat of mixing. The term within the bracket is responsible for enhancing the diffusion coefficient and is known as Darken term.

However, in cases where a chemical reaction also occurs at the interface of growing mixed layer, the reaction rate can strongly influence the concentration gradients and thus can become the dominant source of thermodynamically controlled modification of the diffusion coefficient. This effect of reaction kinetics on mass transport coefficients is well known in the analysis of compound forming thermal diffusion couples.^{20–22} Desimoni and Traverse¹ use this analogy with thermal synthesis of compounds in explaining ion-beam mixing results for silicides.

This is best illustrated by considering a bilayer system A/B , where each layer is an infinite source of corresponding atoms; and for simplicity let only one atom, say A , be the moving species during compound formation. Assume that the solubility of A and B is very low, but they are highly reactive resulting into a compound $A_a B_b$. On irradiation, initially the rate of the growth of the layer $A_a B_b$ is limited by the rate of reaction. However, at later times the supply of the mobile species to the reacting interface gets limited by its diffusion through the mixed layer.¹ If the reaction rate is high, then each atom arriving at the interface is consumed in the formation of the compound, and hence for the steady-state growth, the flux of mobile atoms due to diffusion must equal the flux participating in the formation of the compound at the interface. Assuming a small layer of thickness X , this equality of steady-state flux F_s can be written as¹

$$F_s = D \frac{(C_A - C_i)}{X} = k C_i, \quad (2)$$

where C_A is the atomic density of layer A and C_i is the concentration of A atoms at the growing interface, k is the reaction rate, and D is the diffusion coefficient. Note that the reaction-rate coefficient determines “reaction kinetics,” which in turn influences “transport kinetics” in a diffusion controlled process. The relationship between kinetics and thermodynamics in phase formation in ion-beam mixing has been discussed by Kelly and Miotello.²³

The time dependence of thickness X of the mixed layer can be expressed as a steady-state flux divided by the concentration of atom A in the compound,

$$\frac{dX}{dt} = \frac{F_s}{N_A} = \Phi \frac{dX}{d\Phi}, \quad (3)$$

where N_A is the concentration of A in the compound $A_a B_b$ with atomic density C , i.e., $N_A = (a/a + b)C$. The second equality is obtained by replacing time by dose assuming the flux Φ to be constant.

Using Eqs. (2) and (3) eliminating C_i and solving for X with initial condition, $X(t=0)=0$, one obtains

$$X = \frac{D}{k} \left[\left(1 + 2D \frac{C_A}{N_A} \frac{\Phi}{\dot{\Phi}} \frac{k^2}{D^2} \right)^{1/2} - 1 \right]. \quad (4)$$

For diffusion-limited process and high reaction rate k , X becomes independent of k giving rise to

$$X^2 = 2 \frac{C_A}{N_A} D \frac{\Phi}{\dot{\Phi}} = D_{\text{eff}} \frac{\Phi}{\dot{\Phi}}. \quad (5)$$

Note that though k does not explicitly appear in this equation, it is responsible for enhancement of D to some D_{eff} by a factor $2C_A/N_A$, the origin of which can be attributed to chemical driving force for the formation of a compound.¹ In the approximation that there is no terminal solid solution, this is the only enhancement factor different from the Darken term in Eq. (1). It is straight forward to extend Eq. (5) to the case when both atomic species are mobile and is given by

$$X^2 = 2 \left[\frac{C_A}{N_A} + \frac{C_B}{N_B} \right] D \frac{\Phi}{\dot{\Phi}}. \quad (6)$$

It is interesting to note that the enhancement factor appears as a ratio of concentration of mobile species to its concentration in the compound and is independent of the deposited energy.¹ However, under irradiation conditions the diffusion coefficient is separately dependent on deposited energy F_D . This dependence is known to vary as F_D^2 in case of overlapping subcascades⁵ and only as F_D in case of nonoverlapping subcascades.^{9,10} In case of nonoverlapping subcascades/local spikes, under a regular solution approximation the mixing rate $x^2/\Phi|_{\text{loc}}$ for the later case is given as¹⁰

$$\left. \frac{X^2}{\Phi} \right|_{\text{loc}} = \frac{k_b Z_{\text{ave}}^{1.77} F_D}{C^{2/3} \Delta H_{\text{coh}}^2} \left[1 + \frac{\Delta H_{\text{mix}}}{\Delta H_{\text{coh}}} \right], \quad (7)$$

where ΔH_{coh} is the average cohesive energy^{5,24} of the mixed elements, and k_b is proportionality constant. The first factor is due to the spike effect and the second one is due to the effect of the chemical driving force. In the case of compound formation, this would be further enhanced by the factor shown in Eqs. (5) or (6) above. However, in the absence of terminal solution, the Darken term can be simply replaced in Eq. (7) by the compound formation enhancement factor^{1,18} in Eq. (6) [or Eq. (5)] and the mixing rate $X^2/\Phi|_{\text{loc}}^{\text{com}}$ would be given by

$$\left. \frac{X^2}{\Phi} \right|_{\text{loc}}^{\text{com}} = K_s \left[\frac{C_A}{a/(a+b)} + \frac{C_B}{b/(a+b)} \right] \frac{2F_D Z_{\text{ave}}^{1.77}}{C^{5/3} \Delta H_{\text{coh}}^2}, \quad (8)$$

where K_s is the proportionality constant. This expression is similar to Eq. (11b) of Ref. 1 for overlapping subcascades. When atom A (B) is the only moving species during phase formation, then the first (second) term within the bracket will be retained.

It is our intention to show the extent of quantitative success of such a phenomenological treatment of compound formation in the presence of local spikes, without seeking to explore the detailed mechanisms at this stage. However, a qualitative understanding leads to a mental picture in which the mobile species is transported to the growing interface where it is consumed in compound formation along with simultaneous structural relaxation.

III. EXPERIMENTAL DETAILS

A number of samples having bilayer configuration were prepared by sequentially depositing high-purity Cu and Ge films onto clean fused quartz substrate without breaking vacuum using an electron-gun evaporation system equipped with a digital thickness monitor to measure the thickness *in situ*. Some samples were prepared with a thin marker layer of

gold of thickness ≤ 20 Å deposited between Cu and Ge layers for studying movement of atoms across the interface during mixing. The total thickness of these bilayer samples was in the range of 150 to 270 nm with an overall composition in the vicinity of $\text{Cu}_{50}\text{Ge}_{50}$.

Ion-beam mixing was done by 1-MeV Kr^+ and Ar^+ from 100 to 373 K for a dose of $(2-20) \times 10^{15}$ at./cm². The incident ion flux was kept low ($\leq 5 \times 10^{12}$ at./cm² s⁻¹) to minimize sample heating. At this energy most of the irradiating ions are transmitted through the bilayer structure. The values of range and deposited energy density F_D by the irradiating ions in the target were calculated using Monte Carlo computer program TRIM.²⁵ The Rutherford backscattering (RBS) measurements with the (1.3–1.5) MeV He^+ beam were carried out to study the composition and growth of the mixed layers. The ion implanted partially passivated detector was mounted at a backscattering angle of 150° subtending a solid angle of 2.57 mSr and the total-energy resolution was 14 keV [full width at half maximum]. The 2-MeV Van de Graaff accelerator at IIT Kanpur was used for both irradiation and RBS measurements. The RUMP code²⁶ has been used to simulate all experimental RBS spectra. The RBS spectra of the mixed samples did not show any noticeable oxygen or carbon concentration. X-ray diffraction measurements have been performed using a $\text{Cu-K}\alpha$ source. The surface morphology has been studied by scanning electron microscopy.

IV. RESULTS

The RBS analysis of the mixed layers for room-temperature irradiation reveals that atomic mixing at the interface has occurred at the lowest dose of 2×10^{15} Kr^+ /cm². At this dose a mixed layer of thickness 160 Å and composition $\text{Cu}_{75}\text{Ge}_{25}$ forms across the interface. The thickness of the mixed layer increases up to a dose of 6×10^{15} Kr^+ /cm². Figure 1(a) shows the RBS spectrum of as-deposited Cu-Ge bilayer sample along with the spectrum taken after ion-beam mixing at a dose of 6×10^{15} Kr^+ /cm². The simulated spectrum (solid line) for the irradiated case is obtained using a layer structure $\text{SiO}_2/\text{Cu}(800 \text{ Å})/\text{Cu}_{75}\text{Ge}_{25}(335 \text{ Å})/\text{Ge}(1410 \text{ Å})$. The effect of Kr irradiation performed at a higher dose of 8×10^{15} Kr^+ /cm² is shown by the RBS spectra of Fig. 1(b). The step in the copper signal at channel number 365 indicates the formation of a stoichiometric composition at the Cu/Ge interface. The simulated spectrum was obtained by using two adjacent layers of the mixed region, one with an overall composition of $\text{Cu}_{75}\text{Ge}_{25}$ and other of composition $\text{Cu}_{83}\text{Ge}_{17}$ is shown by the solid line. The layer structure utilized for simulation was $\text{SiO}_2/\text{Cu}(540 \text{ Å})/\text{Cu}_{83}\text{Ge}_{17}(300 \text{ Å})/\text{Cu}_{75}\text{Ge}_{25}(300 \text{ Å})/\text{Ge}(1350 \text{ Å})$. Similar results are observed for Ar-ion irradiations performed at room temperature. However, the thickness of the mixed region in this case is lower as compared to the one obtained for Kr irradiated samples for the same dose.

Since the thickness of the mixed layer is typically 10–30 nm, the x-ray-diffraction measurements did not clearly show the phases formed after mixing. To get the information about the phases formed we have performed ion-beam mixing of multilayer Cu/Ge samples under similar experimental conditions. In this configuration the mixing occurs at each interface, resulting in an overall larger thickness of the mixed region. We have shown in Ref. 2 that for doses lower than

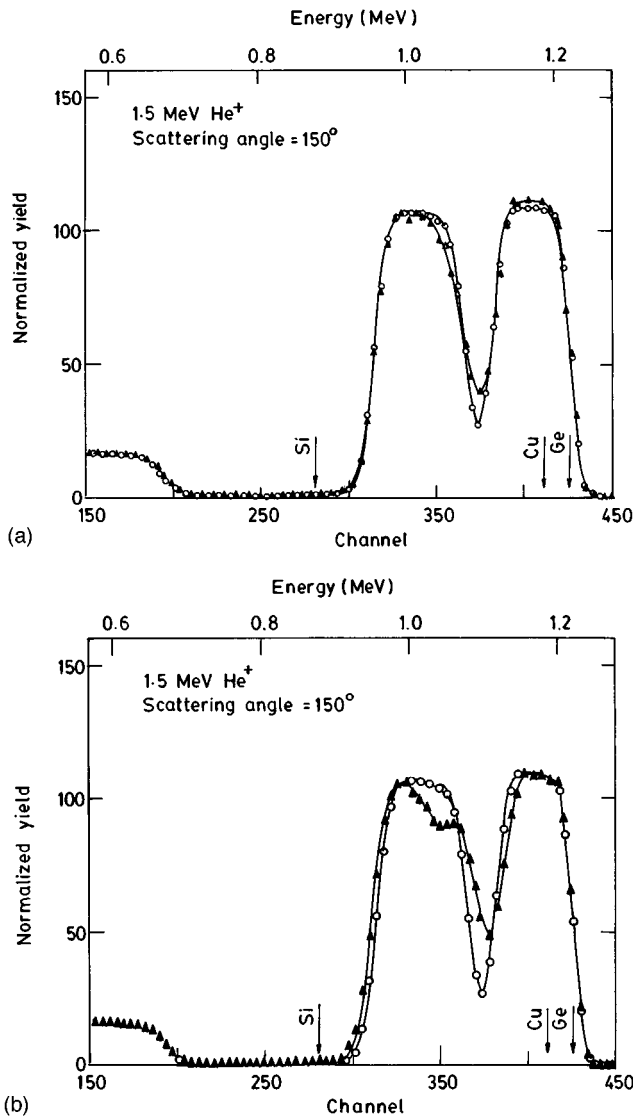


FIG. 1. Rutherford backscattering spectra of a Cu/Ge bilayer on quartz substrate for as deposited sample (○) and after room-temperature mixing (▲) with 1-MeV Kr ions at a dose of (a) 6×10^{15} Kr/cm², (b) 8×10^{15} Kr/cm². The corresponding simulated spectra are shown by solid lines. The arrows show the surface position of different elements.

8×10^{15} Kr⁺/cm² the ϵ_1 -Cu₃Ge phase is formed after mixing, whereas at higher doses the Cu₅Ge phase is formed together with the ϵ_1 phase. In the case of an Ar ion the ϵ_1 -Cu₃Ge phase is formed up to a dose of 1×10^{16} Ar⁺/cm². This sequence of phase formation is consistent with the thermal annealing experiments reported in literature.^{27,28} The surface topography of all samples observed under scanning electron microscope do not show any noticeable features before and after mixing. In this study, we will consider the dose range where growth of only the Cu₃Ge phase occurs.

The squared thickness (X^2) of the mixed layers of the Cu₃Ge phase produced at room temperature, due to both Kr- and Ar-ion bombardment are plotted as a function of dose and are shown in Fig. 2. The linear variation of X^2 with the dose for both cases suggests that the mixing is like a diffusion controlled process. Similar behavior has also been reported for the phase formation in this system by thermal

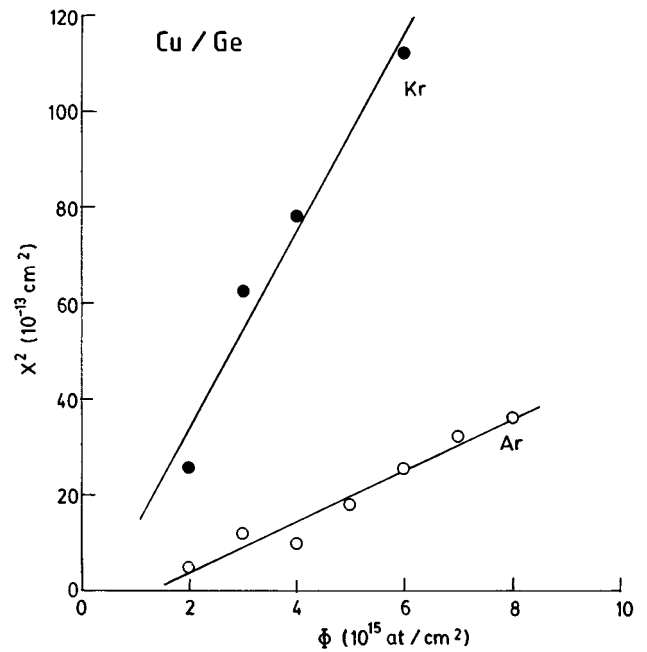


FIG. 2. Dose dependence of squared thickness of mixed layers of composition Cu₃Ge formed across the interface of Cu/Ge bilayer system irradiated at room temperature with 1-MeV Ar ions (○) and Kr ions (●), respectively.

growth, where X^2 varies linearly with time.²⁷ In fact, the linear dependence of X^2 is a general trend that has been found in ion-beam mixing and thermal annealing experiments in many metal/silicon^{1,4} and metal/metal^{3,5,8-10} systems. From these dose dependence studies (Fig. 2), the value of mixing rates (X^2/Φ) at room temperature are found to be 20.6 and 5.4 nm⁴ for Kr- and Ar-ions bombardment, respectively. The dependence of the mixing rate on the deposited energy density F_D at the interface can be studied from the plot of mixing rate as a function of F_D , which is shown in Fig. 3. It is clearly seen from Fig. 3 that the mixing rate is linearly proportional to F_D . Similar behavior has been re-

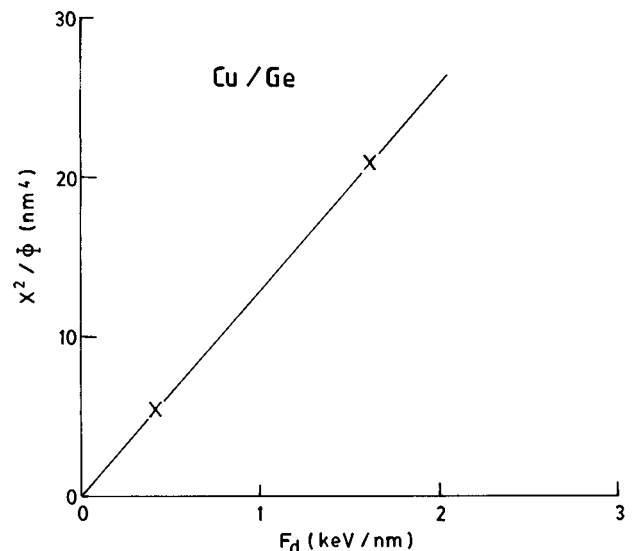


FIG. 3. The variation of the mixing rate measured in Cu/Ge bilayer system for different deposited energy F_D at the interface.

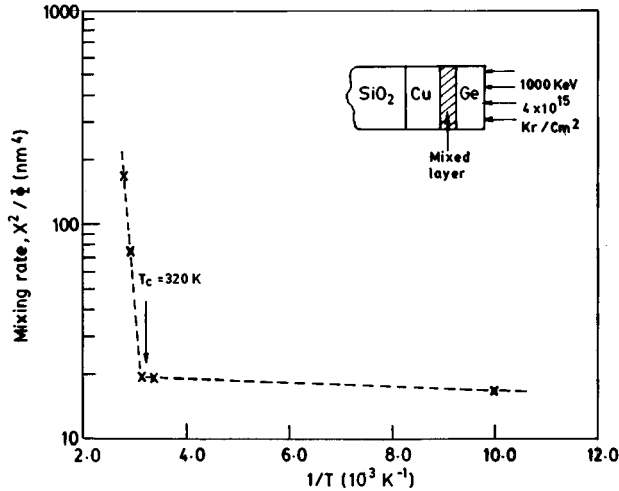


FIG. 4. The variation of the mixing rate for a Cu/Ge bilayer system as a function of reciprocal of substrate temperature for a dose of 4×10^{15} Kr/cm².

ported for many medium-*Z* metal/metal systems.^{9,10} The slope of this linear dependence gives a mixing efficiency ($X^2/\Phi F_D$) of 13.1 nm⁵/keV. This mixing parameter is a useful measure of the ion mixing rate, since it normalizes the mixed thickness to deposited energy, thereby providing a convenient means to compare results on different systems performed under different irradiation conditions.

The temperature dependence of the mixing rate (normally referred to as the *Q* curve) for Kr irradiation is depicted in Fig. 4. This figure clearly shows that the mixing is nearly temperature independent up to 328 K, with a steep increase at higher temperatures. The critical temperature, which marks the beginning of the temperature-dependent mixing, is about 320 K. It is to be noted that for this system, the formation of the equilibrium phase after thermal treatment has been observed above 373 K.^{19,28} We have also performed ion-beam mixing experiments using Ar ions and the mixing does not exhibit a sharp temperature dependence as in the case of Kr. The values of the mixing rates in the case of Ar are lower for similar doses, but the critical temperature does not change appreciably. The activation energy for the temperature-dependent part calculated from Fig. 4 for Kr irradiation is around 1 eV, which is close to the one reported for thermal diffusion.²⁷

V. DISCUSSIONS

Before proceeding to quantitative comparison of the mixing rate predicted by different models, we show that occur-

rence of nonoverlapping subcascades is indeed expected in the present experiments. Recently, Bolse¹⁰ has suggested that the transition from local to global spike mixing occurs above the critical energy density F_D^{cri} , which depends on the atomic number of both the irradiating ion and target atoms. The calculation¹⁰ shows that the value of F_D^{cri} for this system is about 2.60 keV/nm. As the deposited energies in the present experiment for incident Kr and Ar ions are less than the critical value as compared in Table I, it is expected that the mixing should occur under local spikes. The linear F_D scaling has been found for many metal/metal and metal/silicon systems for which the ratio of heat of mixing (ΔH_{mix}) and cohesive energy (ΔH_{coh}) varies in the range of $0 < \Delta H_{\text{mix}}/\Delta H_{\text{coh}} < 0.2$ (Figs. 2 and 3 of Ref. 9). For these systems, Borgesen, Lilienfeld, and Johnson⁹ and Bolse¹⁰ separately have suggested on the basis of their series of experimental results that the linear dependence of the mixing rate with F_D can be correlated with the formation of local spikes. Our experimental results also show a linear dependence of mixing rate with F_D (Fig. 3) and the value of this ratio $\Delta H_{\text{mix}}/\Delta H_{\text{coh}}$ for Cu/Ge system is 0.01.

The role of thermal spike in phase formation has been underlined by several authors. For example, Hamdi and Nicolet²⁹ have concluded through their experimental observations for silicide growth by ion-beam mixing that a thermal spike mixing is the likely mechanism, because radiation enhanced diffusion cannot readily account for the similarity between the thermally activated and ion-induced phase formation sequence. Similar conclusion have been made by Collins, Edwards, and Dearnaley³⁰ from their experimental value of activation energy for the Co/Si system by considering the temperature of spike.

We first consider the model presented in this paper to calculate the mixing rates. In order to determine the compound formation factor in Eq. (8), it is essential to know whether only one of them or both species are mobile during the formation and growth of the Cu₃Ge phase. In order to investigate this, we have studied the movement of atomic species across the interface during mixing by marker experiments. From the analysis of RBS spectra obtained from these marker experiments, we have found that both Cu and Ge move across the interface to form the copper germanide phase with Cu as the dominant moving species. Thermal annealing²⁸ experiments performed with the marker layer at the interface also show that for temperatures below 573-K the copper atom is the dominant moving species, and above this temperature both species are mobile. In ion beam mixing, the atomic movement occurs during the cooling stage of the thermal spike. Since the local temperature of the spike is normally very high,³ both Cu and Ge move to form the com-

TABLE I. The values of the average atomic number Z_{ave} , atomic density C , heat of formation ΔH_{for} (Ref. 2), cohesive energy ΔH_{coh} (Refs. 5, 24), displacement energy E_d (Ref. 31), deposited energy density F_D (Ref. 25), and critical energy F_D^{cri} for the global spike (Ref. 10) of the Cu/Ge and Ni/Si systems.

Bilayer system	Z_{ave}	C in at./Å ³	$-\Delta H_{\text{for}}$ (kJ/g at.)	$-\Delta H_{\text{coh}}$ (eV/at.)	E_d (eV)	Irradiating ion	F_D (keV/nm)	F_D^{cri} (keV/nm)
Cu/Ge	30.5	0.075	4	3.67	17	Ar	0.4	2.6
						Kr	1.6	
Ni/Si	21	0.078	16	4.5	20	Au	4.8	5.5

TABLE II. Comparison between experimental ($X^2/\Phi|^{exp}$) and calculated mixing rates. The theoretical mixed rates ($X^2/\Phi|_{loc}^{com}$) calculated from our model [Eq. (8)] agree well with the experimentally obtained mixing rates. Note the significant departures of the rates calculated from modified ballistic [Eq. (9)] model ($X^2/\Phi|_{bal}^{com}$) and global spike ($X^2/\Phi|_{glo}^{com}$) model [Eq. (11b) of Ref. 1].

Bilayer system	Phase formed	Moving species	F_D (keV/nm)	$X^2/\Phi ^{exp}$ (nm ⁴)	$X^2/\Phi _{loc}^{com}$ (nm ⁴) Eq. (8)	$X^2/\Phi _{bal}^{com}$ (nm ⁴) Eq. (9)	$X^2/\Phi _{glo}^{com}$ (nm ⁴) Eq. (11b) of Ref. 1
Cu/Ge	Cu ₃ Ge	both	0.4	5.4	5.36	0.49	0.25
Cu/Ge	Cu ₃ Ge	both	1.6	20.6	21.46	1.96	4.0
Ni/Si	Ni ₂ Si	Ni	4.8	11.8	8.92	2.04	9.27

pound during ion-beam mixing.

The value of mixing rate for the Cu/Ge system calculated [Eq. (8)] from our model is 21.46 and 5.36 nm⁴ for Kr- and Ar-ion bombardment, respectively. The parameters used for these calculation are given in Table I. These calculated values together with experimental values in the nearly temperature-independent region are compared in Table II. The mixing efficiency calculated from our model is 13.4 nm⁵/keV, which is close to the experimental one and is compared in Table III.

Now we shall compare the experimental mixing rate with the calculated one from the ballistic model,¹⁵ since it also predicts the linear variation of mixing rate with F_D . According to Desimoni and Traverse,¹ the ballistic mixing rate $X^2/\Phi|_{bal}^{com}$ can be written as

$$\frac{X^2}{\Phi}|_{bal}^{com} = \left[\frac{C_A}{a/(a+b)} + \frac{C_B}{b/(a+b)} \right] \frac{0.4F_D\mu^{1/2}\lambda^2}{C^2E_d}, \quad (9)$$

where E_d is displacement energy, μ is the reduced mass, and $\lambda=10$ Å is the minimum separation distance for the formation of stable Frenkel pair.⁵ Using $E_d=20$ eV (Ref. 31), this expression gives mixing rates of 0.49 and 1.96 nm⁴ for Ar- and Kr-ion irradiation, respectively. These values are also given in Table II for comparison. It is clearly seen from Table II that mixing rates calculated from our model are very close to the experimental mixing rates whereas mixing rates from the ballistic model are one order of magnitude less than the experimental values, which suggests that the local spike mechanism is dominant over the collisional one. For completeness, the calculated mixing rates from the Eq. (11b) of

TABLE III. Comparison between experimental ($X^2/\Phi F_D|^{exp}$) and calculated mixing efficiencies. The theoretical mixing efficiency ($X^2/\Phi F_D|_{loc}^{com}$) calculated from our model agree well with the experimentally obtained mixing efficiency. The mixing efficiencies for modified ballistic [Eq. (9)] model ($X^2/\Phi F_D|_{bal}^{com}$) and global spike ($X^2/\Phi F_D|_{glo}^{com}$) model (Ref. 1) are also shown for comparison.

Bilayer system	$X^2/\Phi F_D ^{exp}$ (nm ⁵ /keV)	$X^2/\Phi F_D _{loc}^{com}$ (nm ⁵ /keV)	$X^2/\Phi F_D _{bal}^{com}$ (nm ⁵ /keV)	$X^2/\Phi F_D _{glo}^{com}$ (nm ⁵ /keV)
Cu/Ge	13.1	13.4	1.23	1.56
Ni/Si	2.46	1.86	0.42	1.93

Ref. 1 are also shown in the Table II although it predicts F_D^2 dependence with the mixing rate. Clearly, our model provides the best agreement with the experimental results. The mixing efficiencies calculated from these two models are also compared with the experimental one in Table III.

Desimoni and Traverse¹ have done mixing experiments on Ni/Si system to produce the nickel silicide (Ni₂Si) phase and explained the experimentally obtained mixing rate by the modified global spike model for compound formation.¹ Since the Ni/Si system consists of medium Z_{ave} elements, it is expected that the model proposed here is appropriate to explain the mixing rates in this case as well. In this system, Ni is the only moving species¹ during the nickel silicide phase (Ni₂Si) formation hence only the first term in the compound formation factor [Eq. (8)] is to be considered. The calculated mixing rate from our model and experimental mixing rate for the low temperature reported in Ref. 1 are in close agreement as shown in Table II, whereas the ballistic one is about four times less than that of the experimental one. The experimental and calculated mixing efficiencies are compared in Table III.

It is to be noted that we have used the same average value of the proportionality constant $K_s=0.95$ Å³ eV [Eq. (8)] in our model for calculating the mixing rates for all the three cases. In general, these results suggest that this model might be able to predict the high mixing rates for other compound medium- Z_{ave} systems, where local spike models^{9,10} are inadequate. There are many systems in this category for which phase formation has been reported in the literature. Unfortunately, the information regarding mixing rates for compound formation for these systems are not available. The knowledge of mixing rate will be helpful for further validation of the proposed model.

Finally, it is important to discuss the nature of the final mixed region on the basis of the Q curve presented in Fig. 4. In general, there exists two critical temperatures T_c and T_{eq} with $T_c < T_{eq}$ such that metastable phases are expected between T_c and T_{eq} and equilibrium phases are expected above T_{eq} . de Reus *et al.*¹² have correlated these temperatures with the energies required for creating a hole due to the smaller and the larger element in the compound. The smaller hole formation energy is related with T_c , while the larger one is related with T_{eq} . Also, Cheng *et al.*¹⁴ have correlated T_c with cohesive energy while Rossi and Nastasi¹¹ have correlated it with the melting temperature. In several systems, the

difference between T_c and T_{eq} is not so pronounced and in those cases there is only one transition temperature.¹² For the present case of the Cu/Ge system (Fig. 4) the value of T_c is 320 K. Theoretically, the models of de Reus, Rossi and Nastasi, and Cheng *et al.* give T_c values of 253, 347, and 373 K, respectively. According to the formulation of de Reus *et al.*,¹² the value of T_{eq} is 330 K. This comparison of calculated T_c and T_{eq} values with the experimental results is reasonably well. However, we have observed the formation of the equilibrium Cu_3Ge phase in our experiments performed at room temperature and above. It may be noted that even at very low temperatures, structurally simple phases have been observed after ion irradiation.^{3,32} Also, several silicides form around T_c , which could be due to the higher reactivity of these materials as compared with the metal-metal systems. For example, for the Co-Si system, the experimental²⁹ and theoretical¹² values of T_c and T_{eq} are both equal to 300 K. In this case, the formation of equilibrium phase Co_2Si is reported to occur at room temperature under Xe ion bombardment.²⁹ In fact, there are many more systems where an equilibrium phase is formed around T_c . In the case of the Ni/Ge (Ref. 33) system, $T_c=338$ K and $T_{eq}=455$ K, but the equilibrium phase Ni_2Ge forms at room temperature. Similarly for the Pd/Ge system³⁴ for which $T_c=371$ K and $T_{eq}=383$ K, the equilibrium Pd_2Ge phase forms at 300 K. Several such examples are reported in Refs. 32, 35, etc. Also note that the experimentally determined T_c values show a dependence on the mass of the irradiated ion^{11,30} in several cases.

The growth of mixed layers at relatively low temperatures for highly reactive systems, such as silicides and germanides, must be viewed differently from those systems where a solid solution or amorphous phase is produced under ion irradiation prior to the formation of equilibrium compounds. In the later case, long-range atomic migration or the overcoming of the barrier to nucleation is necessary.³ However, in reacting systems where the diffusive flux of the reacting species is controlled by the reaction rate k , such barriers are either absent or negligible so that the system undergoes structural

relaxation producing a stable equilibrium compound.¹ The role of ion irradiation is to provide the required flux of reacting species for incorporation into the compound at the reacting interface. Hence models such as the one presented here and of Desimoni and Traverse would be of general applicability for systems with a high reaction-rate coefficient and low solid solubility.

VI. CONCLUSIONS

We summarize as follows.

(1) A model has been proposed for medium- Z_{ave} elements, where compound formation occurs during ion-beam mixing under nonoverlapping subcascades. In this model the mixing rate is enhanced by the compound formation factor in highly reactive systems, and it inherits the linear dependence of deposited energy density of nonoverlapping subcascades.

(2) For the Cu/Ge system, we have shown that the growth of the mixed layer is like a diffusion controlled process and the mixing rate exhibits a linear dependence with deposited energy density, F_D . The room-temperature mixing rates are found to be 5.4 and 20.6 nm⁴ for Ar- and Kr-ion bombardment, respectively. The mixing efficiency is independent of the deposited energy density and is found to be 13.1 nm⁵/keV. The critical temperature is around 320 K and above this strong temperature dependence has been observed.

(3) An excellent agreement has been obtained between the experimental results and calculated values from our proposed model for Cu/Ge as well as in Ni/Si systems.

ACKNOWLEDGMENTS

The authors are grateful to Professor R. M. Singru and Professor V. A. Singh for constant encouragement and also to T. Som, P. K. Giri, B. Bhattacharya, K. Ramakrishnan, and the technical staff of the Van de Graaff laboratory of IIT, Kanpur for help during different experimental measurements.

*Electronic address: sankar@iitk.ernet.in

†Electronic address: ynm@iitk.ernet.in

‡Electronic address: vnk@iitk.ernet.in

¹J. Desimoni and A. Traverse, Phys. Rev. B **48**, 13 266 (1993).

²S. Dhar, T. Som, Y. N. Mohapatra, and V. N. Kulkarni, Appl. Phys. Lett. **67**, 1700 (1995).

³M. Nastasi and J. W. Mayer, Mater. Sci. Eng. R **12**, 1 (1994).

⁴A. H. Reader, A. H. van Ommen, P. J. W. Weijs, R. A. M. Wolters, and D. J. Oostra, Rep. Prog. Phys. **56**, 1397 (1992).

⁵Y.-T. Cheng, Mater. Sci. Rep. **5**, 45 (1990).

⁶T. L. Alford, P. Borgesen, J. W. Mayer, and D. A. Lilienfeld, Appl. Phys. Lett. **58**, 1848 (1991).

⁷W. L. Johnson, Y.-T. Cheng, M. Van Rossum, and M.-A. Nicolet, Nucl. Instrum. Methods Phys. Res. Sect. B **7/8**, 657 (1985).

⁸P. Borgesen, D. A. Lilienfeld, and H. Msaad, Nucl. Instrum. Methods Phys. Res. Sect. B **59/60**, 563 (1991).

⁹P. Borgesen, D. A. Lilienfeld, and H. H. Johnson, Appl. Phys. Lett. **57**, 1407 (1990).

¹⁰W. Bolse, Nucl. Instrum. Methods Phys. Res. Sect. B **80/81**, 137 (1993).

¹¹F. Rossi and M. Nastasi, J. Appl. Phys. **69**, 1310 (1991).

¹²R. de Reus, A. M. Vredenberg, A. C. Voorrips, H. C. Tissing, and F. W. Saris, Nucl. Instrum. Methods Phys. Res. Sect. B **53**, 24 (1991).

¹³L. E. Rehn and P. R. Okamoto, Nucl. Instrum. Methods Phys. Res. Sect. B **39**, 104 (1989).

¹⁴Y.-T. Cheng, X.-A. Zhao, T. Banwell, T. W. Workman, M.-A. Nicolet, and W. L. Johnson, J. Appl. Phys. **60**, 2615 (1986).

¹⁵P. Sigmund and A. Gras-Marti, Nucl. Instrum. Methods Phys. Res. Sect. B **182/183**, 25 (1981).

¹⁶H. Gades and H. M. Urbassek, Phys. Rev. B **51**, 14 559 (1995).

¹⁷R. Kelly and A. Miotello, Appl. Phys. Lett. **64**, 2649 (1994).

¹⁸J. Desimoni and A. Traverse, Nucl. Instrum. Methods Phys. Res. Sect. B **80/81**, 91 (1993).

¹⁹M. O. Aboelfotoh, C. L. Lin, and J. M. Woodall, Appl. Phys. Lett. **65**, 3245 (1994).

²⁰U. Gosele and K. N. Tu, J. Appl. Phys. **53**, 3252 (1982).

²¹U. Gosele and K. N. Tu, J. Appl. Phys. **66**, 2619 (1989).

²²S. W. Russell and S. Q. Wang, J. Appl. Phys. **76**, 264 (1994).

²³R. Kelly and A. Miotello, Thin Solid Films **241**, 192 (1994).

- ²⁴C. Kittel, *An Introduction to Solid State Physics* (Wiley, New York, 1976).
- ²⁵J. F. Ziegler, J. P. Biersack, and U. Littmark, *The Stopping and Range of Ions in Solids* (Pergamon, New York, 1986), Vol. 1.
- ²⁶L. R. Doolittle, Nucl. Instrum. Methods Phys. Res. Sect. B **9**, 344 (1985).
- ²⁷S. Q. Hong, C. M. Comrie, S. W. Russell, and J. W. Mayer, J. Appl. Phys. **70**, 3655 (1991).
- ²⁸F. M. d'Heurle and J. Gupta, Appl. Surf. Sci. **73**, 214 (1993).
- ²⁹A. H. Hamdi and M.-A. Nicolet, Thin Solid Films **119**, 357 (1984).
- ³⁰R. A. Collins, S. C. Edwards, and G. Dearnaley, J. Phys. D **24**, 1822 (1991).
- ³¹H. H. Andersen, Appl. Phys. **18**, 131 (1979).
- ³²T. Weber and K. P. Lieb, J. Appl. Phys. **73**, 3499 (1993).
- ³³E. Jaroli, N. Q. Khanh, G. Mezey, E. Zsoldos, B. Kovacs, I. Mojzes, T. Lohner, E. Kotai, A. Manuaba, M. Fried, and J. Gyulai, Nucl. Instrum. Methods Phys. Res. Sect. B **15**, 703 (1986).
- ³⁴J. Li, Q. Z. Hong, and J. W. Mayer, J. Appl. Phys. **66**, 3600 (1989).
- ³⁵F. Shi, W. Bolse, and K. P. Lieb, J. Appl. Phys. **78**, 2303 (1995).